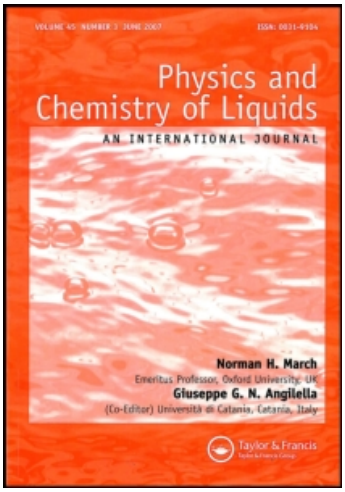


**Physics and Chemistry of Liquids**
Publication details, including instructions for authors and subscription information:
http://www.informaworld.com/smpp/title~content=t713646857

# Pressure-induced structural and dynamic transitions in stimulated liquid aluminosilicate nanoparticles

Nguyen Ngoc Linh[ab]; Ngo Huynh Buu Trong[b]; Vo Van Hoang[b]; Tran Thi Thu Hanh[b]
[a] Scuola Internazionale Superiore di Studi Avanzati, 3014 Trieste, Italy [b] Department of Physics, Institute of Technology, National University of HoChiMinh, HoChiMinh, Vietnam

Online publication date: 27 January 2011

**To cite this Article** Linh, Nguyen Ngoc , Huynh Buu Trong, Ngo , Van Hoang, Vo and Thi Thu Hanh, Tran(2011) 'Pressure-induced structural and dynamic transitions in stimulated liquid aluminosilicate nanoparticles', Physics and Chemistry of Liquids, 49: 1, 81 — 90
**To link to this Article: DOI:** 10.1080/00319101003596089
**URL:** http://dx.doi.org/10.1080/00319101003596089

*Physics and Chemistry of Liquids*
Vol. 49, No. 1, January 2011, 81–90

Taylor & Francis
Taylor & Francis Group

# Pressure-induced structural and dynamic transitions in stimulated liquid aluminosilicate nanoparticles

Nguyen Ngoc Linh[ab]*, Ngo Huynh Buu Trong[b], Vo Van Hoang[b] and Tran Thi Thu Hanh[b]

[a]*Scuola Internazionale Superiore di Studi Avanzati, via Beirut 2–4, 3014 Trieste, Italy;* [b]*Department of Physics, Institute of Technology, National University of HoChiMinh, 268 Ly Thuong Kiet, District 10, HoChiMinh, Vietnam*

(*Received 28 October 2009; final version received 5 January 2010*)

We have investigated the pressure-induced structural and dynamic transitions in liquid aluminosilicate ($Al_2O_32SiO_2$) nanoparticles with a molecular dynamics (MD) method. Simulations were performed in spherical models under non-periodic boundary conditions containing 2596 ions with the Born–Mayer type pair potentials. In order to study the structural and dynamic changes, the models of liquid aluminosilicate nanoparticles have been built at densities ranging from $2.60\,g\,cm^{-3}$, corresponding to the size of 4 nm, to the density of $4.2\,g\,cm^{-3}$ at a temperature of 4200 K. The microstructure of the liquid nanoparticles has been analysed in detail through the coordination number distribution, bond-angle distribution and interatomic distances. We found a clear evidence of transition from the low density state (LDS) to high density state (HDS) structure in the models upon compression, like that observed in the bulk counterparts. This transition is accompanied by an anomalous diffusion of Al and Si atoms in the systems. Moreover, we also show the surface distribution properties in order to highlight the surface effects on dynamics upon compression.

**Keywords:** aluminosilicate nanoparticles; pressure-induced transition; molecular dynamics simulation



## 1. Introduction

Pressure-induced transition has been an important subject in condensed matter physics and material science for a long time. In particular, problems relating to liquid–liquid phase transitions, i.e. occurrence of structural transition under high pressure, have been under intensive investigation by both experiments and computer simulations. Through a variety of research on liquids with bulk phase such as water, silica, carbon, $GeO_2$, $Al_2O_3$ and silicon [1–8], it was found that the transition from low density states (LDS) to high density state (HDS) in network structure liquids with bulk phase is often accompanied by an anomalous diffusion, i.e. the diffusion constant increases with increasing density (or pressure). Analogously, the pressure-induced structure in nanosized substances has aroused great interest

*Corresponding author. Email: nnlinh@sissa.it

ISSN 0031–9104 print/ISSN 1029–0451 online

DOI: 10.1080/00319101003596089
http://www.informaworld.com

because the mechanism of structural transition in the finite size systems, compared with the bulk, can be different from their analogues in the bulk counterparts, i.e. the finite size systems can have richer metastable structures due to the surface effects. Recently, X-ray diffraction measurements for nanometre-sized silica particles have exhibited inelastic compression between 4 and 8 GPa, in which the anomalous compressive behaviour of fumed silica results from a decreased compressibility of nanoparticles [9]. In addition, the liquid–liquid phase transitions were related to the soft-core interaction potential systems such as gallium confined droplets, which showed a clear change in the absorption in the liquid phase obtained between 0 and 1.6 GPa, and it indicates that transformations involving microscopic structure and/or electronic states occur [10]. Also, for the higher pressures, i.e. between 2.7 and 5.8 GPa, the quantity of crystallised gallium droplets increases as a function of pressure [10]. Furthermore, the pressure-induced phase transition from ice to water in the confined geometry was found by *ab initio* molecular dynamics (MD) simulation. The study showed the breaks and the reforms of the H bonds corresponding to the changes of the self-diffusion coefficients during phase transition process that occurred in the simulated model [11]. Since there is no general rule to determine the pressure-induced phase transition at nano-scaled materials, it is hard to avoid any artifact involved in the experiments and simulation. Thus, it is really necessary to develop a study in this direction.



On the other hand, the study of property changes in liquid aluminosilicates under pressure is also of fundamental importance in both the earth and materials sciences, in which structure, evolution and dynamics of aluminosilicate systems at extremely high pressures are related to magma flows inside the Earth. Therefore, the structure and diffusion in this system under high pressure have been investigated in detail by computer simulation and experiment. Indeed, by using $^{27}$Al solid-state NMR spectrometry, pressure-induced transition from tetrahedral to octahedral unit structures for Al coordination has been evidenced in liquid aluminosilicates [12]. Similarly, more details about the structural and dynamic transitions of this system have also been studied by computer simulation in our previous work. A clear evidence of transition from a tetrahedral to an octahedral network structure was found in the model, accompanied by an anomalous diffusion of components in the system upon compression, similar to that observed in simple oxide systems [13]. However, there is no study related to the same transition in liquid aluminosilicate nanoparticles. It raises a question as to whether these behaviours still exist in the liquid phase of finite size systems in which a periodical boundary condition does not apply, i.e. in the liquid aluminosilicate nanoparticles.

The lack of results also motivated us to carry out the comprehensive study on the structural and dynamic transitions of liquid aluminosilicate spherical models under high pressure in order to highlight other features of liquid–liquid phase transitions in this nanoscaled material.

## 2. Calculations

MD simulations were carried out of initial spherical liquid aluminosilicate nanoparticles with a diameter of 3 nm under non-periodic boundary conditions.

The models contain 2596 atoms (including Al, Si and O). We use the empirical interatomic potentials of the Born–Mayer type, which have the form given below:

$$U_{ij} = z_i z_j \frac{e^2}{r} + B_{ij} \exp\left(-\frac{r}{R_{ij}}\right), \quad (1)$$

where the first term represents Coulomb and the second, repulsion energies, respectively. Here, $r$ denotes the distance between the centers of $i$th and $j$th ions; $Z_i$ and $Z_j$ the charges of $i$th and $j$th ions; $B_{ij}$ and $R_{ij}$ the parameters accounting for the repulsion of the ionic shells. Values $Z_{Al} = +3, Z_{Si-O} = +4$ and $Z_O = -2$ are the charges of $Al^{+3}$, $Si^{+4}$ and $O^{-2}$, respectively. We use the values $B_{Al-Al} = 0\,eV$, $B_{Al-O} = 1779.86\,eV$, $Z_{Al-O} = 4.10$, $B_{Si-Si} = 0\,eV$, $B_{Si-O} = 1729.50\,eV$, $B_{O-O} = 1500\,eV$ and $R_{ij} = 29\,pm$. We found that interatomic potentials (Equation (1)) described well both structure and dynamics of liquid and amorphous aluminosilicate nanoparticles compared with those obtained by experiment [14–15]. The Coulomb interactions were taken into account by means of Ewald–Hansen method. The equilibrated melt at 7000 K has been obtained by relaxing a random configuration for 50,000 MD steps. We use the Verlet algorithm and MD time step is of 1.6 fs. The system was cooling down from the melt at constant volume corresponding to the high density of $2.6\,g\,cm^{-3}$. The temperature of the system was decreased linearly in time as $T = T_o - \gamma t$, with the cooling rate $\gamma = 4.375 \times 10^{13}\,K s^{-1}$ to a temperature of 4200 K in order to obtain the properties of liquid nanoparticle models upon compression and compare them to those observed in the compression process of the bulk counterpart [13]. The models have been built at different densities ranging from $2.6\,g\,cm^{-3}$ to $4.0\,g\,cm^{-3}$ at a constant temperature of 4200 K. The volume of the spheres is reduced isotropically step-by-step corresponding to the density increment of $0.2\,g\,cm^{-3}$. The systems are thermalised for 100,000 MD steps (or 160 ps) to reach an equilibrium liquid state at each constant density (e.g. at constant volume) before calculating the static and dynamic properties. Calculated data have been averaged over two independent runs for increasing statistics. In order to calculate the coordination number and bond-angle distributions in the models, we adopt the fixed values $R_{Al-Al} = 3.80\,Å$, $R_{Al-Si} = 3.70\,Å$, $R_{Si-Si} = 3.50\,Å$, $R_{Al-O} = 2.60\,Å$, $R_{Si-O} = 2.50\,Å$, $R_{O-O} = 3.70\,Å$. Here, $R$ is the cut-off radius, which was chosen as the position of the minimum after the first peak in $g_{ij}(r)$ for the amorphous model at ambient pressures like those used in Ref. [14]. These cut-off radii were chosen as the first minimum after the first peak in the corresponding partial radial distribution functions (PRDFs).



## 3. Results and discussion

### 3.1. *Structural evolution of liquid aluminosilicate nanoparticles upon compression*

In order to obtain an evolution of the structure upon compression, we have studied the structural characteristics of well-relaxed models at different densities ranging from 2.6 to $4.0\,g\,cm^{-3}$ at a constant temperature of 4200 K. Calculations, as presented in Tables 1–3 and Figures 1 and 2, show that the structural evolution in the liquid nanoparticles shares a similar trend as that observed in the bulk counterpart upon compression. Namely, the distance of Al–O and Si–O pairs increases, as found in the bulk [13], with the increase of density while for other pairs it decreases; the

Table 1. Mean interatomic distance, $r_{ij}$ (in Å) and bond-angle distributions, $\theta_{ijk}$, for different atomic pairs in liquid aluminosilicate nanoparticle models upon compression.

| Density ($g\,cm^{-3}$) | $P$ (GPa) | $r_{ij}$ (Å) | | | | | | $\theta_{ijk}$ | | | |
|---|---|---|---|---|---|---|---|---|---|---|---|
| | | Al–Al | Al–Si | Si–Si | Al–O | Si–O | O–O | O–Al–O | Al—O–Al | O–Si–O | Si–O–Si |
| 2.6 | 2.69 | 3.13 | 3.11 | 3.06 | 1.65 | 1.50 | 2.52 | 103.23 | 113.88 | 107.68 | 147.20 |
| 2.8 | 4.21 | 3.11 | 3.11 | 3.05 | 1.66 | 1.50 | 2.52 | | | | |
| 3.0 | 6.06 | 3.10 | 3.09 | 3.04 | 1.67 | 1.50 | 2.51 | | | | |
| 3.2 | 8.14 | 3.09 | 3.09 | 3.03 | 1.69 | 1.51 | 2.49 | 99.45 | 110.48 | 105.51 | 137.84 |
| 3.4 | 10.70 | 3.07 | 3.08 | 3.02 | 1.70 | 1.51 | 2.48 | | | | |
| 3.6 | 13.67 | 3.06 | 3.06 | 3.02 | 1.70 | 1.51 | 2.46 | | | | |
| 3.8 | 17.54 | 3.04 | 3.05 | 3.02 | 1.71 | 1.52 | 2.44 | | | | |
| 4.0 | 22.79 | 3.03 | 3.04 | 3.02 | 1.72 | 1.53 | 2.43 | 94.84 | 107.67 | 102.89 | 126.21 |

Table 2. Mean coordination number, $Z_{ij}$, for different atomic pairs in liquid aluminosilicate nanoparticle models upon compression.

| Density ($g\,cm^{-3}$) | $Z_{ij}$ | | | | | | | | |
|---|---|---|---|---|---|---|---|---|---|
| | Al–Al | Al–Si | Si–Al | Si–Si | Al–O | O–Al | Si–O | O–Si | O–O |
| 2.60 | 3.44 | 2.67 | 2.81 | 2.28 | 4.01 | 1.58 | 4.08 | 1.37 | 8.47 |
| 2.80 | 3.66 | 2.94 | 3.03 | 3.29 | 4.27 | 1.63 | 4.18 | 1.39 | 9.06 |
| 3.00 | 3.85 | 3.03 | 3.09 | 2.51 | 4.35 | 1.69 | 4.27 | 1.41 | 9.55 |
| 3.20 | 3.99 | 3.22 | 3.27 | 2.64 | 4.49 | 1.70 | 4.35 | 1.46 | 10.04 |
| 3.40 | 3.88 | 3.55 | 3.63 | 2.66 | 4.67 | 1.70 | 4.50 | 1.46 | 10.57 |
| 3.60 | 3.98 | 3.78 | 3.82 | 2.88 | 4.79 | 1.72 | 4.68 | 1.51 | 11.11 |
| 3.80 | 4.19 | 3.95 | 4.01 | 3.08 | 5.03 | 1.78 | 4.78 | 1.54 | 11.52 |
| 4.00 | 4.40 | 4.29 | 4.30 | 3.25 | 5.21 | 1.79 | 4.95 | 1.57 | 12.05 |



Table 3. Coordination number distribution for Al–O and Si–O pairs.

| Density ($g\,cm^{-3}$) | $Z_{Al–O}$ | | | | | | | $Z_{Si–O}$ | | | | | | |
|---|---|---|---|---|---|---|---|---|---|---|---|---|---|---|
| | 1 | 2 | 3 | 4 | 5 | 6 | 7 | 1 | 2 | 3 | 4 | 5 | 6 | 7 |
| 2.60 | 2 | 3 | 77 | 224 | 102 | 19 | 0 | 0 | 1 | 12 | 412 | 44 | 3 | 0 |
| 2.80 | 0 | 0 | 96 | 188 | 156 | 30 | 2 | 0 | 0 | 13 | 366 | 89 | 4 | 0 |
| 3.00 | 0 | 1 | 112 | 184 | 160 | 40 | 2 | 0 | 1 | 33 | 304 | 113 | 14 | 0 |
| 3.20 | 0 | 0 | 82 | 181 | 177 | 52 | 4 | 0 | 1 | 20 | 289 | 153 | 13 | 1 |
| 3.40 | 0 | 2 | 40 | 162 | 186 | 70 | 12 | 0 | 1 | 8 | 262 | 165 | 39 | 0 |
| 3.60 | 0 | 0 | 25 | 159 | 187 | 91 | 10 | 0 | 0 | 6 | 208 | 191 | 75 | 2 |
| 3.80 | 0 | 0 | 18 | 110 | 165 | 125 | 24 | 0 | 1 | 3 | 160 | 226 | 102 | 2 |
| 4.00 | 0 | 0 | 6 | 87 | 150 | 148 | 27 | 0 | 1 | 4 | 117 | 246 | 165 | 2 |

decrease of Si–Si, Si–O and O–O pairs has been obtained identically in previous *in situ* high-pressure diffraction experiments on the silica nanoparticles. The experiment also states that within the range of pressure from 4 to 8 GPa, the configurations of the constituent $SiO_4$ tetrahedral units slightly change, which is similar to the mechanical transformation upon compression of the bulk counterpart

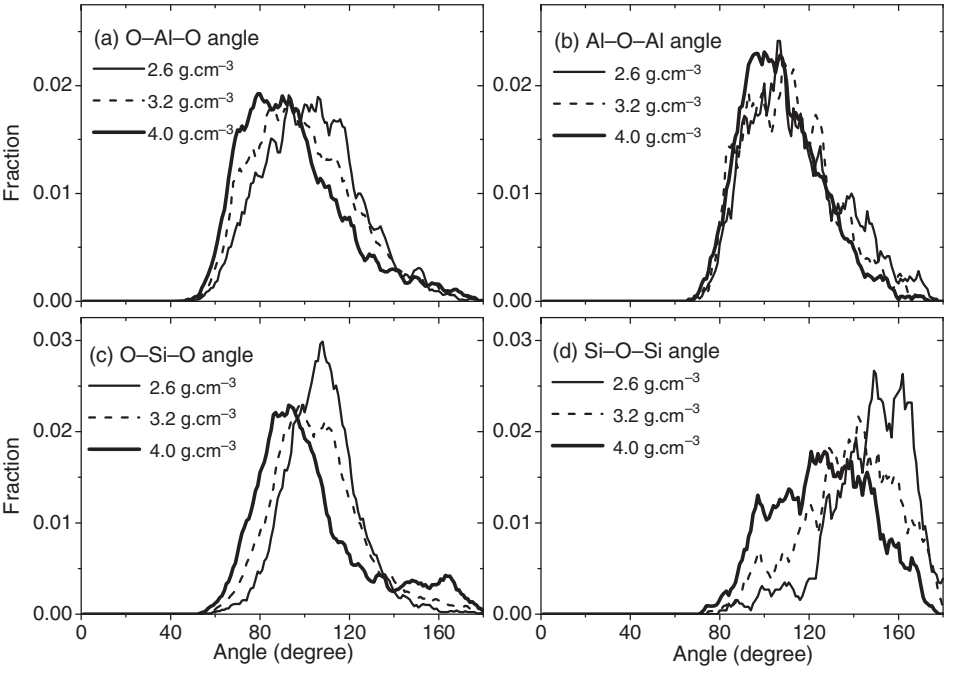


Figure 1. Bond-angle distributions of aluminosilicate nanoparticles at 4200 K and at different densities.

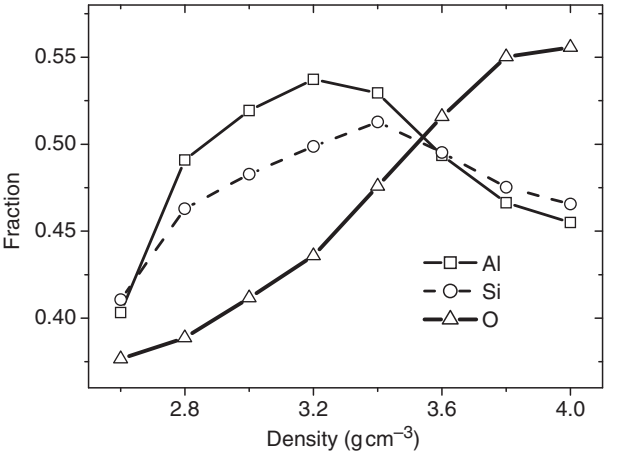


Figure 2. The ratio of the number of each atomic species at the surface per total number of atomic species, i.e. $N_{\mathrm{Al}}^{(\mathrm{surf.})}/N_{\mathrm{Al}}^{(\mathrm{total})}$, $N_{\mathrm{Si}}^{(\mathrm{surf.})}/N_{\mathrm{Si}}^{(\mathrm{total})}$ and $N_{\mathrm{O}}^{(\mathrm{surf.})}/N_{\mathrm{O}}^{(\mathrm{total})}$, upon compression.

[9]. Analogously, in our calculation, the mean coordination number for all atomic pairs increases with increase in density, which indicates the formation of a more close-packing structure in the system. In addition, the bond-angle distributions have been calculated for the most important angles such as O–Al–O, Al–O–Al, O–Si–O

and Si–O–Si, and compared to those of the bulk. We see that upon compression the main peaks of the curves shifted towards smaller angles in accordance with the close-packing structure at high densities. At a low density of 2.60 g cm$^{-3}$, the main peak of O–Al–O and O–Si–O angle distributions is centered at 103° and 108°, respectively, and at a high density of 4.00 g cm$^{-3}$ the values are at 94° and 103°, respectively. Moreover, we find that at the LDS, 2.6 g cm$^{-3}$, the liquid aluminosilicate nanoparticles have a slightly distorted tetrahedral network structure with the mean coordination numbers $Z_{Al-O} = 4.10$ and $Z_{Si-O} = 4.08$, and these values are locally similar to the local structure of the liquid aluminosilicate observed in the bulk counterpart, but at higher density states, 4.00 g cm$^{-3}$, a new structure is formed with the mean coordination numbers $Z_{Al-O} = 5.21$ and $Z_{Si-O} = 4.95$, and these values correspond to those of a slightly distorted pentahedral network structure.

On the other hand, from Table 3, one can also find that upon compression the fraction of high-coordinated Al (or Si) atoms to oxygen, i.e. $Z_{Al,\,Si-O} = 5$ and 6, increases while the fraction of low-coordinated Al (or Si) atoms to oxygen, i.e. $Z_{Al,\,Si-O} = 4$, decreases. This trend is the same as that observed in the bulk counterpart. However, in nanoparticles the change of the fractions of low-coordinated atoms is gradual, and even at a high density such as 4.0 g cm$^{-3}$, the fractions of low-coordinated atoms are still high. In contrast, compared with the pressure-induced phase transition in the liquid states of the bulk models, a structural transition from a tetrahedral to an octahedral network structure takes place completely at around 3.00 or 3.20 g cm$^{-3}$ [13]. It means that the transition density (or transition pressure) in the liquid aluminosilicate nanoparticles is higher than that for the bulk counterpart. It has been argued through the studies in crystal nanoparticles that as the crystallite size becomes smaller, the shape change at the phase transformation involves making higher index planes that are unstable. As a consequence, the transition pressure increases [16]. In contrast, it should be pointed out that in the liquid nanoparticles there may be other factors, such as defects and finite volume effects, that contribute to the elevation in transition pressure. The result in our work is explained similarly to that found in pressure-induced structural transitions in the amorphous state of nanoparticles [17], in which the difference between phase transition in liquid nanoparticles and their bulk counterpart is estimated by the effects of the surface of nanoparticles, i.e. breaking bonds at the surface reduces a large number of structural defects found in nanoparticles [18]. Indeed, as presented in Table 3, we find that the fraction of low-coordinated atoms, i.e. $Z_{Al,\,Si-O} = 3$, is higher and changes more significant than that observed for the bulk. This fraction increases with increasing density from 2.6 to 3.4 g cm$^{-3}$ and then it decreases at higher densities. In addition, following our previous work, the fraction of low-coordinated atoms has a significant role in the formation of structure defects at the surface of the aluminosilicate nanoparticles [18]. Thus, from Figure 2, it is essential to note that the change in the number of Al and Si atoms at the surface corresponds to the change in the mean coordination number of $Z_{Al,\,Si-O} = 3$ shown in Table 3. Meanwhile, the number of oxygen atoms at the surface increases gradually. In order to highlight this result, two snapshots of aluminosilicate nanoparticles at 3.2 and 4.00 g cm$^{-3}$ have been shown in Figure 3. Overall, it is quite reasonable to conclude that upon compression from the melts the distribution of atoms in the nanoparticles is different for every different species of atom, i.e. the number of Al and Si atoms in the surface shell of the liquid

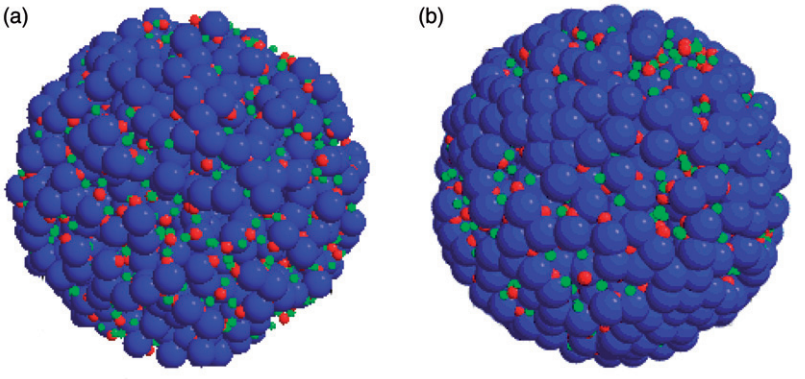


Figure 3. Snapshots of the aluminosilicate nanoparticle at densities of 3.2 (a) and 4.0 g cm$^{-3}$ (b). The biggest blue spheres are the oxygen atoms, the smaller red spheres are the silicon atoms and the smallest green spheres are aluminum atoms (colour online).



aluminosilicate nanoparticles increases with density and then it decreases at the higher densities, while the number of oxygen atoms increases continuously with increasing density. This phenomenon reflects the corresponding change not only in the mass density and in the concentration of defects in the surface of the nanoparticles but it also effects on the changes of dynamic properties of atoms upon compression, and more details will be shown in the next part of this article.

### 3.2. *Pressure-induced dynamic transition in liquid aluminosilicate nanoparticles*

It is known that the liquid–liquid phase transition in network liquids is often accompanied by an anomalous diffusion of components in the bulk system. However, this problem has not been investigated yet for the nano-scaled systems such as the liquid aluminosilicate nanoparticles. In this work, the self-diffusion constant $D$ of particles in nanoparticles was calculated via the Einstein relation

$$D = \lim_{t\to\infty} \frac{\langle r^2(t)\rangle}{6t},$$

where $\langle r^2(t)\rangle$ is the mean-squared atomic displacement. The time dependence of $\langle r^2(t)\rangle$ for Al, Si and O particles belonging to the core of the liquid aluminosilicate nanoparticles at a density of 4.0 g cm$^{-3}$ is shown in Figure 4(a). Moreover, the time dependence of $\langle r^2(t)\rangle$ for particles in the surface shell of nanoparticles is considered in Figure 4(b). One can see clearly that the pressure-induced dynamic transitions for oxygen atoms are quite different between in the core and in the surface shell of nanoparticles in that the mean-squared atomic displacement for oxygen at the surface shell are more pronounced at high pressures. Furthermore, the density dependence of diffusion constant, $D$, in liquid aluminosilicate nanoparticles, presented in Figure 5, has been investigated with an anomalous behaviour of the diffusion constants of Al and Si particles, i.e. they have a maximum at around the density of 3.20 g cm$^{-3}$, which is similar to those observed previously in liquid $H_2O$,

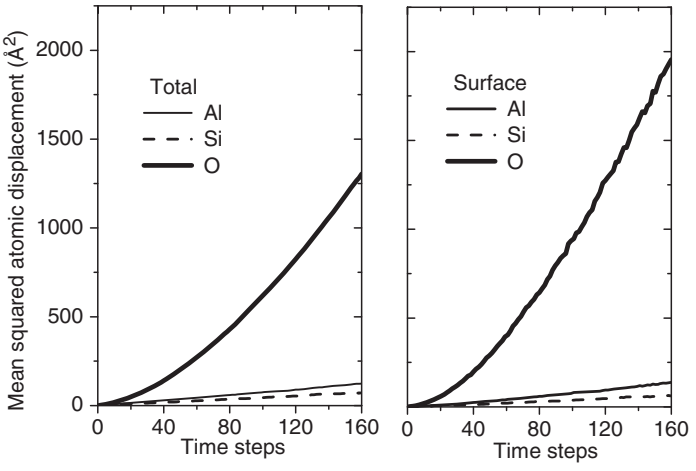


Figure 4. Mean-squared atomic displacement of atomic species in aluminosilicate nanoparticles obtained in averaged total and at surface nanoparticles.



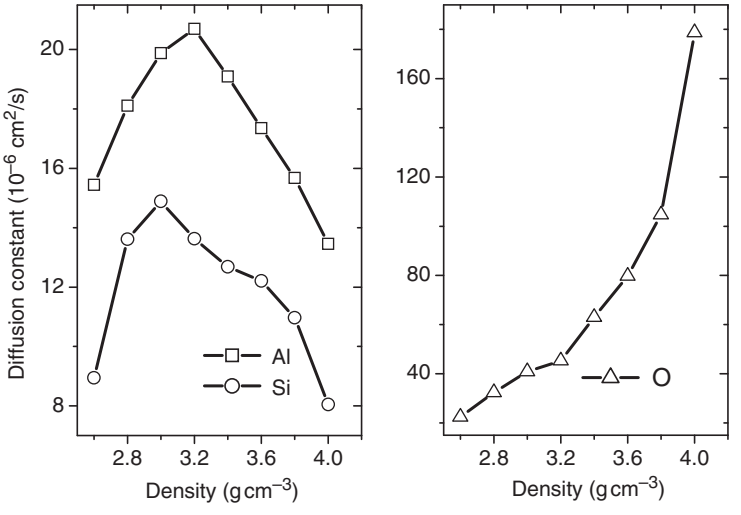


Figure 5. Density dependence of diffusion constants of Al and Si atoms (left) and oxygen atoms (right) upon compression.

$SiO_2$ and in the bulk of aluminosilicate [13,19,20]. It has been considered that anomalous diffusion observed in water and Si results from the competition of the following two mechanisms [21]:

(1) the breakdown of the tetrahedral network structure leading to the increase of atomic mobility,
(2) the packing effects by densification leading to the decrease of atomic mobility.

However, the calculations show that the anomalous diffusivity for Al and Si atoms in the liquid aluminosilicate nanoparticles might be explained in a different

way in which the behaviour of the change in the diffusivity of Al and Si atoms is dependent upon the change of the fraction of threefold coordinators with increasing density. From Table 3 we can see that upon compression from 2.60 to 3.20 $g\,cm^{-3}$, the tetrahedral network structure of nanoparticles breaks down gradually (i.e. the number of fourfold-coordinated Al or Si atoms to O decreases) and then the broken atoms have a trend towards moving to the outer surface of the nanoparticles. This is very reasonable since the surface has more defects and the existence of these structural defects in the liquid and amorphous nanoparticles might enhance the diffusion of atomic species at the surface [22–24]. It explains the increase in the diffusivities for Al, Si and O atoms in the liquid aluminosilicate nanoparticles with increasing density from 2.60 to 3.20 $g\,cm^{-3}$. On the other hand, upon further compression, i.e. when the density is larger than 3.2 $g\,cm^{-3}$, the system is completely transformed to a high density state in nanoparticles with the packing effect dominate for Al and Si atoms in the core in which the number of fivefold- and sixfold-coordinated Al and Si atoms to O forms and the domination of Oxygen atoms in the surface shell (Table 3 and Figure 2). Therefore, the diffusion constant for Al and Si atoms strongly decreases with increasing density, and in contrast, the diffusion constant for oxygen atoms increases continuously.



## 4. Conclusions

By using MD simulation, we have found the LDS $\rightarrow$ HDS transition in liquid aluminosilicate nanoparticles in both structural and dynamic properties. Several conclusions can be drawn as follows:

(1) upon compression, a clear evidence of transition from a tetrahedral to a pentahedral network structure in liquid aluminosilicate nanoparticles has been found;
(2) such transition density (or transition pressure) in liquid aluminosilicate nanoparticles is higher than that for the bulk counterpart;
(3) calculation has also shown that, upon compression, the number of Al and Si atoms in the surface changes corresponding to the change in anomalous diffusion of Al and Si atoms; in contrast, this effect was not found for oxygen atoms.

## Acknowledgements

This work was supported by the HoChiMinh City Department of Science and Technology and the Youth Scientific and Technological Development Centre, through the programme 'Support for Development of Young Engineers and Scientists'.

## References

[1] J.R. Rustad, D.A. Yuen, and F.J. Spera, Phys. Rev. A **42**, 2081 (1990).
[2] S. Tsuneyuki and Y. Matsui, Phys. Rev. Lett. **74**, 3197 (1995).
[3] J.N. Glosli and F.H. Ree, Phys. Rev. Lett. **82**, 4659 (1999).
[4] J.R. Errington and P.G. Debenedetti, Nature (London) **409**, 318 (2001).
[5] M.S. Shell, P.G. Debenedetti, and A.Z. Panagiotopoulos, Phys. Rev. E **66**, 011202 (2002).

[6] G. Gutierrez and J. Rogan, Phys. Rev. E **69**, 031201 (2004).
[7] V.V. Hoang, Phys. Lett. A **335**, 439 (2005).
[8] T. Morishita, Phys. Rev. E **72**, 021201 (2005).
[9] T. Uchino, A. Sakoh, M. Azuma, S. Kohara, M. Takahashi, M. Takano, and T. Yoko, Phys. Rev. B **67**, 092202 (2003).
[10] S. Meng, E.G. Wang, and S. Gao, J. Phys.: Condens. Matter **16**, 8851 (2004).
[11] R. Poloni, S. Panfilis, A.D. Cicco, G. Pratesi, E. Pricipi, A. Trapananti, and A. Filipponi, Phys. Rev. B **71**, 184111 (2005).
[12] E. Ohtani, F. Taulelle, and C.A. Angell, Nature **314**, 78 (1985).
[13] V.V. Hoang, N.H. Hung, and N.N. Linh, Phys. Scr. **74**, 697 (2006).
[14] N.N. Linh and V.V. Hoang, Mol. Simul. **34**, 29 (2008).
[15] N.N. Linh and V.V. Hoang, NANO: Brief Reports and Reviews **2**, 227 (2007).
[16] S.B. Qadri, J. Yang, B.R. Ratna, E.F. Skelton, and J.Z. Hu, Appl. Phys. Lett. **69**, 2205 (1996).
[17] V.V. Hoang, J. Phys. D Appl. Phys. **40**, 754 (2007).
[18] N.N. Linh and V.V. Hoang, J. Phys. Condens. Matter **20**, 265005 (2008).
[19] J.R. Errington and P.G. Debenedetti, Nature (London) **409**, 318 (2001).
[20] S. Tsuneyuki and Y. Matsui, Phys. Rev. Lett. **74**, 3197 (1995).
[21] T. Morishita, Phys. Rev. E **72**, 021201 (2005).
[22] D.A. Litton and S.H. Garofalini, J. Non-Cryst. Solids **217**, 250 (1997).
[23] I.V. Schweigert, K.E.J. Lehtinen, M.J. Carrier, and M.R. Zachariah, Phys. Rev. B **65**, 235410 (2002).
[24] A. Winkler, J. Horbach, W. Kob, and K. Binder, J. Chem. Phys. **120**, 384 (2004).